Selective Electroanalysis of Ascorbic Acid Using a Nickel Hexacyanoferrate and Poly(3,4-ethylenedioxythiophene) Hybrid Film Modified Electrode

Tsung-Hsuan Tsai,[a] *Tse-Wei Chen*,[a,b] *Shen-Ming Chen*[a]*

[a] Electroanalysis and Bioelectrochemistry Lab, Department of Chemical Engineering and Biotechnology, National Taipei University of Technology, No.1, Section 3, Chung-Hsiao East Road, Taipei 106, Taiwan (ROC), Tel: (886)-2-27017147, Fax: (886)-2-27025238
[b] Department of Chemistry, Soochow University, 70 Linhsi Road, Shihlin, Taipei 111, Taiwan (ROC)
*e-mail: smchen78@ms15.hinet.net

Received: December 15, 2009
Accepted: February 6, 2010

Abstract
The mixed-valent nickel hexacyanoferrate (NiHCF) and poly(3,4-ethylenedioxythiophene) (PEDOT) hybrid film (NiHCF-PEDOT) was prepared on a glassy carbon electrode (GCE) by multiple scan cyclic voltammetry. The films were characterized using atomic force microscopy, field emission scanning electron microscopy, energy dispersive spectroscopy, X-ray diffraction, and electrochemical impedance spectroscopy (AC impedance). The advantages of these films were demonstrated for the detection of ascorbic acid (AA) using cyclic voltammetry and amperometric techniques. The electrocatalytic oxidation of AA at different electrode surfaces, such as the bare GCE, the NiHCF/GCE, and the NiHCF-PEDOT/GCE modified electrodes, was determined in phosphate buffer solution (pH 7). The AA electrochemical sensor exhibited a linear response from 5×10^{-6} to 1.5×10^{-4} M ($R^2 = 0.9973$) and from 1.55×10^{-4} to 3×10^{-4} M ($R^2 = 0.9983$), detection limit $= 1 \times 10^{-6}$ M, with a fast response time (3 s) for AA determination. In addition, the NiHCF-PEDOT/GCE was advantageous in terms of its simple preparation, specificity, stability and reproducibility.

Keywords: Nickel hexacyanoferrate, PEDOT, Electrocatalysis, Ascorbic acid, Modified electrodes, Thin films, Organic-inorganic hybrid composites

DOI: 10.1002/elan.200900610

1. Introduction

Ascorbic acid (AA) is a vital component in the human diet. In animal organs the highest concentrations of AA are found in the liver, leukocytes, and anterior pituitary lobe. AA is widely used in food and drink to prevent undesirable changes in color and taste, and as an antioxidant [1]. It is found in plant material and the human body, and fruit and vegetables are the major sources of AA in the human diet [2]. AA is also involved in the regulation and synthesis of crucial immune system molecules, such as cytokines, antibodies, and interferon [2]. Recently, it has been found that AA can suppress human immunodeficiency virus (HIV) expression [3] and that it can inhibit the growth of small fragments of human mammary or lung tumors explanted in mice [4–6]. AA also plays an important role in the body as a free radical scavenger, which may help to prevent free radical induced diseases such as cancer and Parkinson's disease. Because of its physical and medical importance, it is essential to develop a rapid, selective, highly efficient, highly stable and renewable AA sensor. Dopamine (DA), AA, and uric acid (UA) usually coexist in human biological systems and are important molecules for physiological processes in human metabolism. Several reports are available on the use of modified electrodes for the simultaneous determination of AA, DA, and UA [7–11]. It is known that the oxidation of AA, DA, and UA takes place at nearly the same potential on a bare electrode, which results in overlapping voltammetric responses, making their discrimination highly difficult [12, 13].

Various analytical methods have been employed for the determination of ascorbic acid, such as spectrophotometry [14, 15], spectrophotofluorimetry [16], atomic absorption spectrometry (AAS) [17], gas chromatography (GC) [18], and high-performance liquid chromatography (HPLC) [19]. The major drawbacks of these methods are that they are highly dependent on laboratory-based techniques that may require slow, and sometimes sophisticated, analytical methodologies [20]. Among these techniques, chemically modified electrodes (CMEs) are available for the detection of ascorbic acid, and they have the characteristics of being simple, stable, and selective, with a short response time and a high sensitivity [7]. Electrochemical techniques are considered very interesting for the determination of AA, DA, and UA owing to their high sensitivity and selectivity.

In recent reports, metal hexacyanoferrates (MHCFs) such as NdHCF [21], AgHCF [22], SnHCF [23], CoHCF [24], NiHCF [25], CuHCF [26], etc., on various electrode

substrates have been used for the determination of AA, DA or UA. MHCFs have also received much attention in many fields because of their special properties and potential applications [27–29].

Poly(3,4-ethylenedioxythiophene) (PEDOT) has been widely investigated as an electronically conducting polymer. It can be easily electrodeposited onto a surface by the electrooxidation of its monomer [30–33]. A PEDOT film in its oxidized form has been found to have high conductivity and stability at physiological pH [34, 35]. NiHCF can be prepared as an electroactive thin film of a Ni substrate in the presence of ferricyanide anions [36, 37]. It is considered to be an attractive material for electrode surface modification owing to its well-defined, reversible, and reproducible responses in supporting electrolytes [38].

The present study is concerned with the effect of a NiHCF-PEDOT hybrid film on electrode behavior and the electrostatic interaction between the NiHCF-PEDOT hybrid film and the ascorbate anion for the following reasons: (i) NiHCF is an efficient mediator for AA oxidation in solution [38], and (ii) PEDOT has also been used to study the electrocatalytic oxidation of AA [34, 35]. Therefore, a composite of NiHCF on a PEDOT film on an electrode's surface may be a novel AA sensor. The interference of DA, UA, acetaminophen (AP), glucose, epinephrine (EP), and H_2O_2 with AA catalysis was studied at the NiHCF-PEDOT/GCE modified electrode. Cyclic voltammetric and amperometric techniques were used to study the mechanism of AA oxidation.

2. Experimental

2.1. Materials

Nickel(II) chloride hexahydrate and 3,4-ethylenedioxythiophene (EDOT) was purchased from Sigma-Aldrich (USA). Double distilled deionized (DDDI) water was used to prepare all solutions. The PEDOT film was prepared by electrochemical polymerization, using 0.2 M $LiClO_4$ as supporting electrolyte. A phosphate buffer solution (PBS, pH 7.0) was prepared using Na_2HPO_4 (0.1 M) and NaH_2PO_4 (0.1 M). Pure nitrogen was passed through all the experimental solutions. All the chemicals used were of analytical grade.

2.2. Apparatus

All electrochemical experiments were performed using a CHI 750a potentiostat (CH Instruments, USA). The Bioanalytical Systems (BAS) glassy carbon electrode (GCE; diameter 0.3 cm, exposed geometric surface area 0.07 cm^2; Bioanalytical Systems, Inc., USA) was used. A conventional three-electrode system was used; it comprised a Ag/AgCl (saturated KCl) reference electrode, NiHCF/GCE and NiHCF-PEDOT/GCE modified electrodes, and a bare GCE electrode, as working electrodes, and platinum wire as counter electrode. Electrochemical impedance studies (EIS) were performed using a ZAHNER impedance analyzer (Germany). The atomic force microscope (AFM) images were recorded using a multimode scanning probe microscope (Being Nano-Instruments CSPM-4000, China). Field emission scanning electron microscope (FE-SEM) images were recorded using a HITACHI S-4700 (Japan). Energy dispersive spectroscopy (EDS) was performed using an Oxford EDS (133 eV (Mn Kα:5.899 keV)). X-ray diffraction (XRD) experiments were carried out using an XPERT-PRO (PANalytical B. V., The Netherlands). Samples were scanned in the range 20–70° (2θ).

2.3. Preparation of Sample and Hybrid Film Modified Electrode

Prior to the electrochemical deposition process the GCE was well polished with aqueous slurries of alumina powder (0.05 μm), using a BAS polishing kit, then rinsed and ultrasonicated in DDDI water. Figure 1A shows the electrodeposition of NiHCF films at the GCE in 0.2 M $LiClO_4$ solution between −0.4 and +1.0 V, at the scan rate of 0.05 V/s for ten cycles. The film formed in aqueous 0.2 M $LiClO_4$ solution had two redox couples [24], with E° values of about +0.42 and +0.59 V. Figure 1B shows the electrochemical polymerization of the NiHCF-PEDOT carried out by the cyclic voltammetric method in 0.2 M $LiClO_4$ solution containing 1×10^{-3} M $K_3Fe(CN)_6$, 1×10^{-3} M $NiCl_2$ and 0.01 M EDOT. The potential cycling was carried out within the potential range of −0.4 and +0.9 V, at the scan rate of 0.05 V/s for ten cycles. The film formed in the aqueous 0.2 M $LiClO_4$ solution had three redox couples, with E° values of about +0.30, +0.45, and +0.59 V. The NiHCF-PEDOT/GCE was washed with deionized water and dried for 5 min. After polymerization, the electrode was treated with 0.1 M PBS (pH 7) solution by repeated cycling in the potential range −0.4 to +1.0 V, at the scan rate of 0.05 V/s, until a stable cyclic voltammogram (CV) was obtained.

3. Results and Discussion

3.1. XRD and EIS Analyses

As shown in Figure 2A, XRD analysis was used to determine the structure of the NiHCF-PEDOT film. The four peaks that appear at around 23.7° (2θ) correspond to the (220) crystallographic plane, the peak at around 32.1° (2θ) corresponds to the (400) plane, the peak at around 37.2° (2θ) corresponds to the (420) plane, and the peak at around 43.4° (2θ) corresponds to the (422) plane (JCPDS 5-0036, 5-0037) [39, 40].

The electrochemical activity of the NiHCF-PEDOT/GCE was examined using the EIS technique. Here the complex impedance can be presented as a sum of the real Z' (ω) and imaginary Z'' (ω) components that originate mainly from the resistance and capacitance of the cell. From the

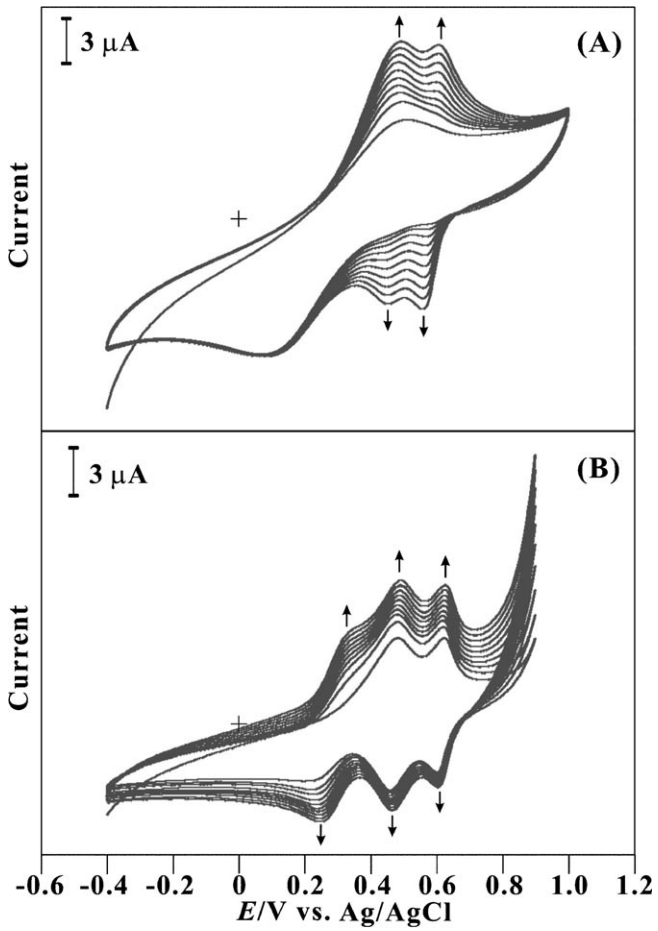

Fig. 1. (A) CVs obtained by consecutive sweeps in a 0.2 M $LiClO_4$ solution containing 1×10^{-3} M $K_3Fe(CN)_6$ and 1×10^{-3} M $NiCl_2$. Potential range −0.4 to 1.0 V. Scan rate 50 mV/s. (B) CVs of consecutive sweeps in a 0.2 M $LiClO_4$ solution containing 1×10^{-3} M $K_3Fe(CN)_6$, 1×10^{-3} M $NiCl_2$, and 0.01 M EDOT. Potential range −0.4 to 0.9 V. Scan rate 50 mV/s.

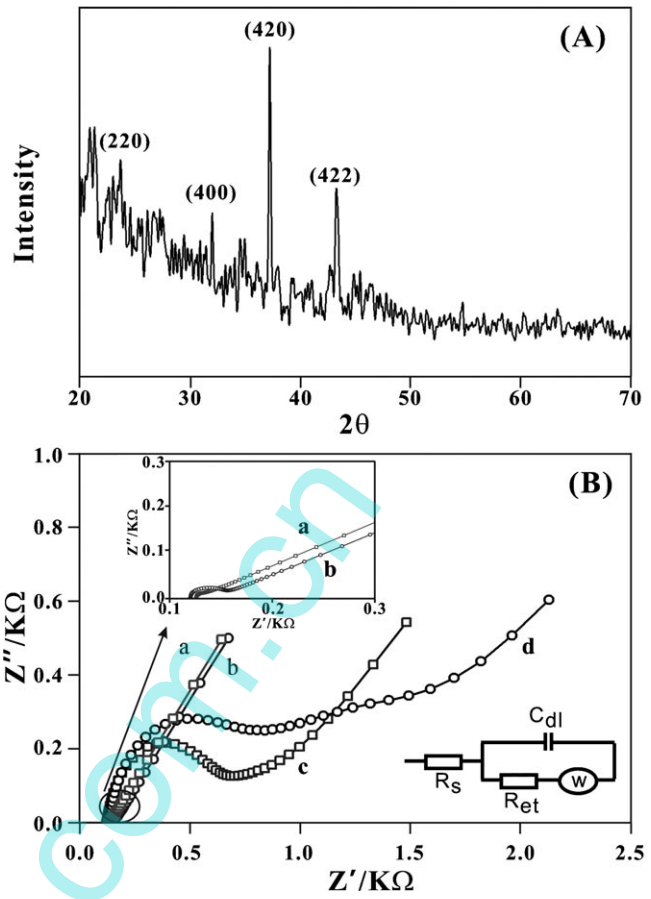

Fig. 2. (A) XRD spectra of a NiHCF-PEDOT film. (B) EIS curves of (a) NiHCF-PEDOT, (b) PEDOT, (c) bare GCE, and (d) NiHCF film modified GCE in 0.1 M PBS (pH 7.0) containing 5×10^{-3} M $K_3[Fe(CN)_6]/K_4[Fe(CN)_6]$ (1:1).

shape of an impedance spectrum, the electron transfer kinetics and diffusion characteristics can be determined. The respective semicircle parameters correspond to the electron transfer resistance (R_{et}) and the double layer capacity (C_{dl}) nature of the modified electrode. As shown in Figure 2B, curve (a) indicates the Nyquist plot of NiHCF-PEDOT/GCE, (b) PEDOT/GCE, (c) bare GCE, and (d) NiHCF/GCE in the presence of 5 mM $K_3[Fe(CN)_6]/K_4[Fe(CN)_6]$ (1:1) in PBS (pH 7.0). The NiHCF-PEDOT/GCE shows a very small depressed semicircle arc with an interfacial resistance due to the electrostatic repulsion between the charged surface and probe molecule $Fe(CN)_6^{3-/4-}$. This depressed semicircle arc ($R_{et} = 0.134$ (Z'/kΩ)) clearly indicates the lower electron transfer resistance behavior compared to that of the bare GCE ($R_{et} = 0.635$ (Z'/kΩ)), the PEDOT/GCE ($R_{et} = 0.155$ (Z'/kΩ)) and the NiHCF/GCE ($R_{et} = 0.804$ (Z'/kΩ)). These results clearly illustrate the electrochemical activities of the NiHCF-PEDOT, PEDOT and NiHCF film modified GCEs, and bare GCE, respectively.

3.2. AFM and SEM Analyses

The surface morphology of the NiHCF-PEDOT hybrid film modified at the GCE electrode and indium tin oxide (ITO) electrode were examined using AFM and FE-SEM. The AFM topography images were determined for a 1300 × 1300 nm surface area. The surface morphology of NiHCF-PEDOT/GCE was examined by using the tapping mode. Figure 3A shows a 2D magnified view of the NiHCF-PEDOT hybrid film modified on the GCE surface. Figure 3B shows a FE-SEM micrograph of the NiHCF-PEDOT hybrid film on an ITO surface. Figure 3C shows the cross-sectional and granularity normal distribution chart of NiHCF-PEDOT particles electrodeposited on the GCE surface. Figure 3D shows EDS results of the NiHCF-PEDOT/GCE. Figure 3A shows that the NiHCF-PEDOT particles have an average size range of 50–120 nm, as also shown in Figure 3C. The average particle diameter of the NiHCF-PEDOT particles was 1.56 nm, and most of the NiHCF-PEDOT particles had a particle diameter of 3.56 nm. Figure 3B shows the FE-SEM images of the NiHCF-PEDOT hybrid film electrodeposited on an ITO surface. PEDOT shows a network structure, with a fiber dimension of 10–20 nm. A polymer network with a highly

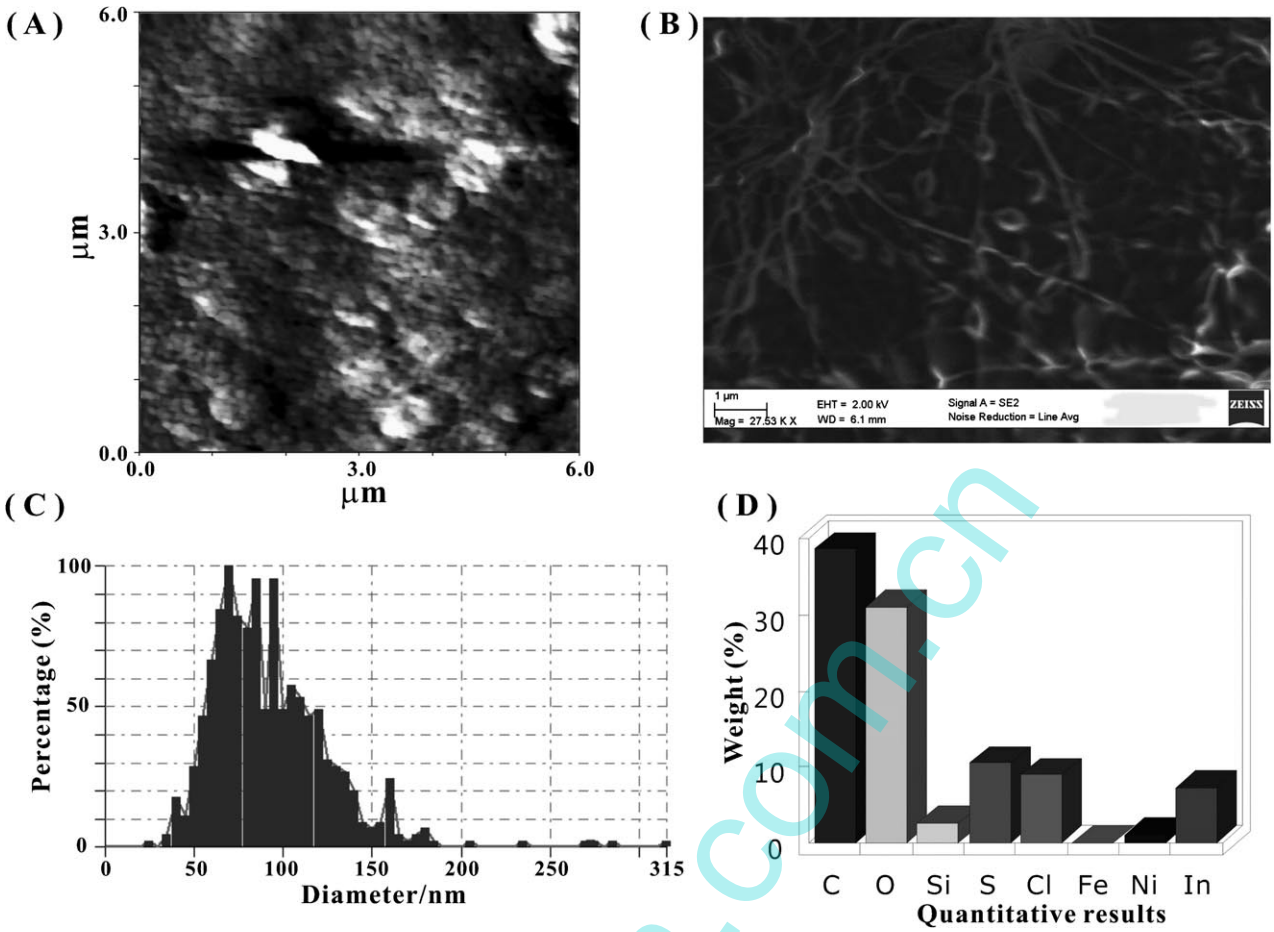

Fig. 3. (A) Tapping mode AFM image (2D) of a NiHCF-PEDOT film on a GCE. (B) FE-SEM image of a NiHCF-PEDOT film on an ITO. (C) AFM cross-sectional analysis graph. (D) EDS analysis of the nano Ag NiHCF-PEDOT film.

porous structure, which might easily entrap NiHCF nanoparticles, can be seen. Further, the EDS spectrum shows that the elements C, O, Si, S, Cl, Fe, Ni, and In are detected in the NiHCF-PEDOT hybrid film modified on ITO electrode. The weight percentages of C (38.07%), O (31.65%), S (3.4%), Cl (8.4%), Fe (0.06%), Ni (0.4%), and In (5.98%) are shown in Figure 3D. The weight percentage ratios of Fe and Ni were electrochemically intercalated/deintercalated with K^+ ions by cyclic voltammetry [41].

3.3. Electrochemical Properties of NiHCF-PEDOT Hybrid Film Modified Electrode

The NiHCF-PEDOT/GCE was used in several scan rate studies in 0.1 M PBS (pH 7.0). Figure 4A exhibits the different scan rate results of NiHCF-PEDOT/GCE in the range 0.1 – 1 V/s. As expected, the CVs of the NiHCF-PEDOT/GCE modified electrodes exhibited a single redox couple with an anodic peak at + 0.458 V and a cathodic peak at + 0.381 V versus Ag/AgCl/KCl_{sat}. Here, the linear increase in the anodic and cathodic peak currents of NiHCF-PEDOT/GCE according to the scan rate revealed that the film exhibited the typical characteristics of a surface-controlled thin-layer electrochemical system. Inset (a) in Figure 4A shows a plot of the NiHCF-PEDOT signal of the anodic and cathodic peak current vs. scan rate. The corresponding linear regression equations were: I_{pa} (µA) = 2.7307v (V/s) + 10.317 (R^2 = 0.991) and I_{pc} (µA) = 2.9863v (V/s) – 9.9584 (R^2 = 0.994). As shown in inset (b) in Figure 4A, the logarithmic form of the peak current vs. scan rate (v) plot yields a gradient of I_{pa} = 0.7778 and I_{pc} = 0.8014, which indicates that the charge transfer was a mixed process with a near-equal contribution from the semi-infinite linear diffusion and surface process [42]. Furthermore, using the electrodeposited film and a follow-up testing process employing an electrochemical buffer solution with different cations [37] led to different electrochemical signals. In a 0.1 M PBS (pH 7.0), the NiHCF/GCE film showed a relatively broad electrochemical signal (Curve b′, Figure 4B), which, when combined with the PEDOT in a modified film, would improve the electrochemical signal, as the redox couple of the NiHCF-PEDOT/GCE system should be sharper.

The electrocatalytic oxidation of AA was investigated using CV (Figure 4B). In Figure 4B, curve (a) indicates the NiHCF-PEDOT/GCE and curve (b′) the NiHCF/GCE modified electrode CV signals. For the NiHCF/GCE

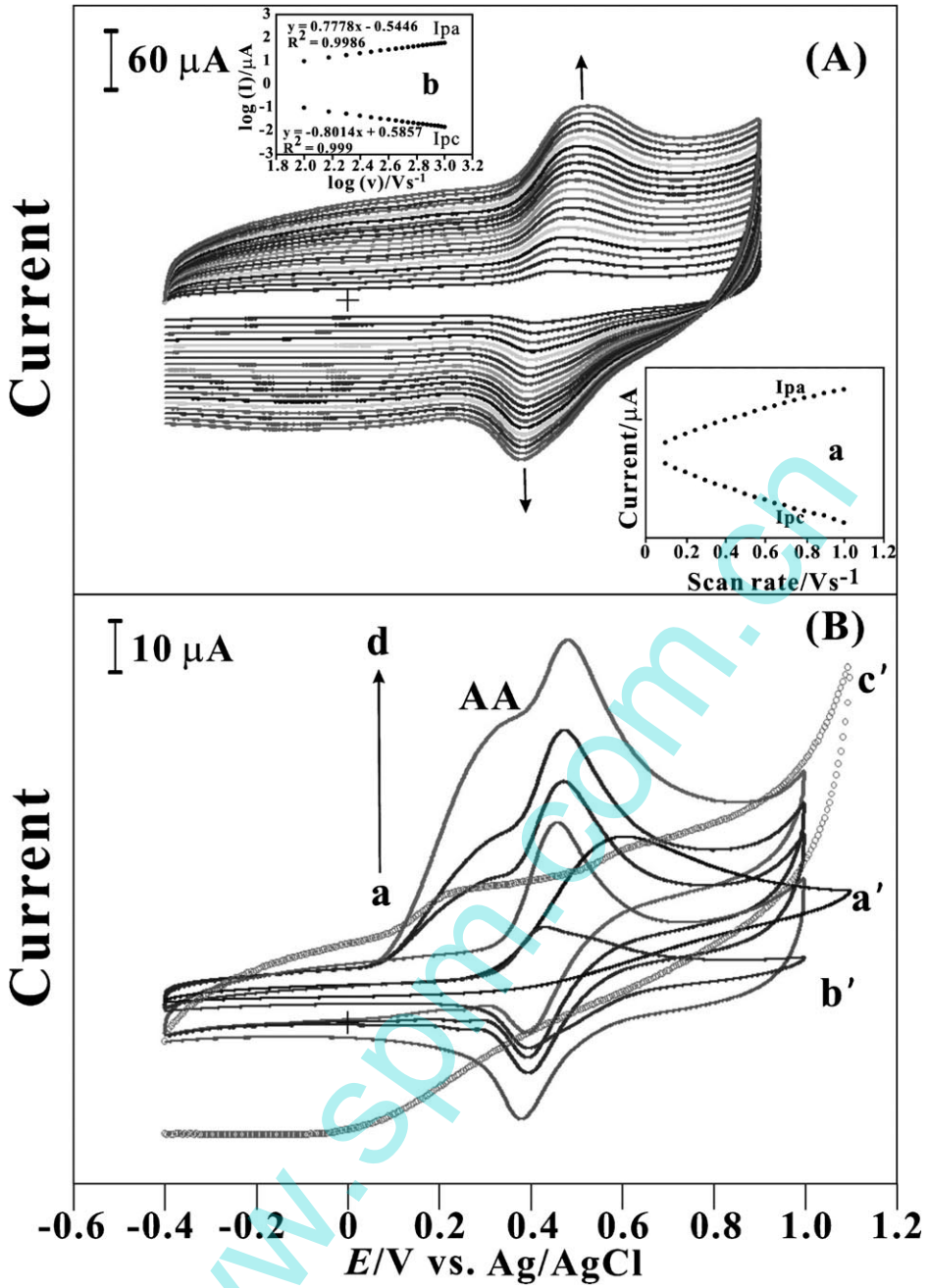

Fig. 4. (A) Results of different scan rate studies of a NiHCF-PEDOT modified GCE in 0.1 M PBS (pH 7.0). Scan rate in the range of a – j: 0.1 – 1 V/s. (B) CVs of NiHCF-PEDOT modified GCE in 0.1 M PBS (pH 7.0): AA (a) 0.0 μM, (b) 25 μM, (c) 50 μM, (d) 100 μM, (a′) bare GCE with 100 μM AA, (b′) NiHCF modified GCE, and (c′) PEDOT modified GCE with 100 μM AA in 0.1 M PBS (pH 7.0). Scan rate = 50 mV/s.

modified electrode, the anodic and cathodic peak currents were significantly lower than observed for the NiHCF/PEDOT modified electrode. The enhanced peak current of NiHCF in the modified electrode is due to the presence of PEDOT. PEDOT offers good stability, high conductivity, and acts as a good matrix. Figure 4B (curves a – d) shows the CVs of the electrochemical oxidation of AA on the NiHCF-PEDOT/GCE and bare GC electrodes for various concentrations of AA in PBS (pH 7). The CVs exhibited a reversible redox couple (anodic peak at about +0.48 V) in the absence of AA. Upon the addition of AA a new oxidation peak of AA appeared at about +0.27 V (vs. Ag | AgCl). An increase in the concentration of AA simultaneously produced an increase in the oxidation current of AA in the NiHCF-PEDOT/GCE peak. This behavior is typical of that expected for the mediated oxidation. Similarly, in Figure 4B, curve (a′) shows the CV signals of a bare GCE electrode, curve (c′) shows the CV signals of a PEDOT/GCE electrode, and curve (d) shows the CV signals of a NiHCF-PEDOT/GCE modified electrode for the same concentra-

tion (10^{-4} M) containing an ascorbic acid buffer solution at pH 7.0. In the same solution, the bare GCE electrode shows a single oxidation peak occurring around +0.58 V, compared with a PEDOT/GCE electrode (+0.232 V) and a NiHCF-PEDOT/GCE electrode (+0.27 V). The bare GCE electrode has the highest oxidation potential in the AA oxidation reaction. The PEDOT/GCE electrode and the NiHCF-PEDOT/GCE electrode have almost the same potential in the AA oxidation reaction, but the peak current of the PEDOT/GCE electrode is much less than that of the NiHCF-PEDOT/GCE electrode. All of the above results indicate that using a NiHCF-PEDOT film modified electrode can help to enhance the electrocatalytic reaction of AA.

3.4. Individual Determination of AA by Amperometry

The amperometric response of the NiHCF-PEDOT hybrid film modified electrode to AA was investigated in a stirred 0.1 M PBS solution (pH 7.0) at a working potential of +0.2 V. Figure 5A shows typical current – time curves for successive additions of AA for different concentrations, between 5×10^{-6} and 3×10^{-4} M, with the NiHCF-PEDOT hybrid film modified electrode. The current immediately changed after the addition of AA and reached another steady-state current within 3 s. The insets a and b in Figure 5A show the calibration curves of a NiHCF-PEDOT hybrid film modified electrode with the concentration of AA between 5×10^{-6} to 1.5×10^{-4} M and 1.55×10^{-4} to 3×10^{-4} M (the correlation coefficients were 0.9973 and 0.9983, respectively). Thus, the present modified electrode shows a

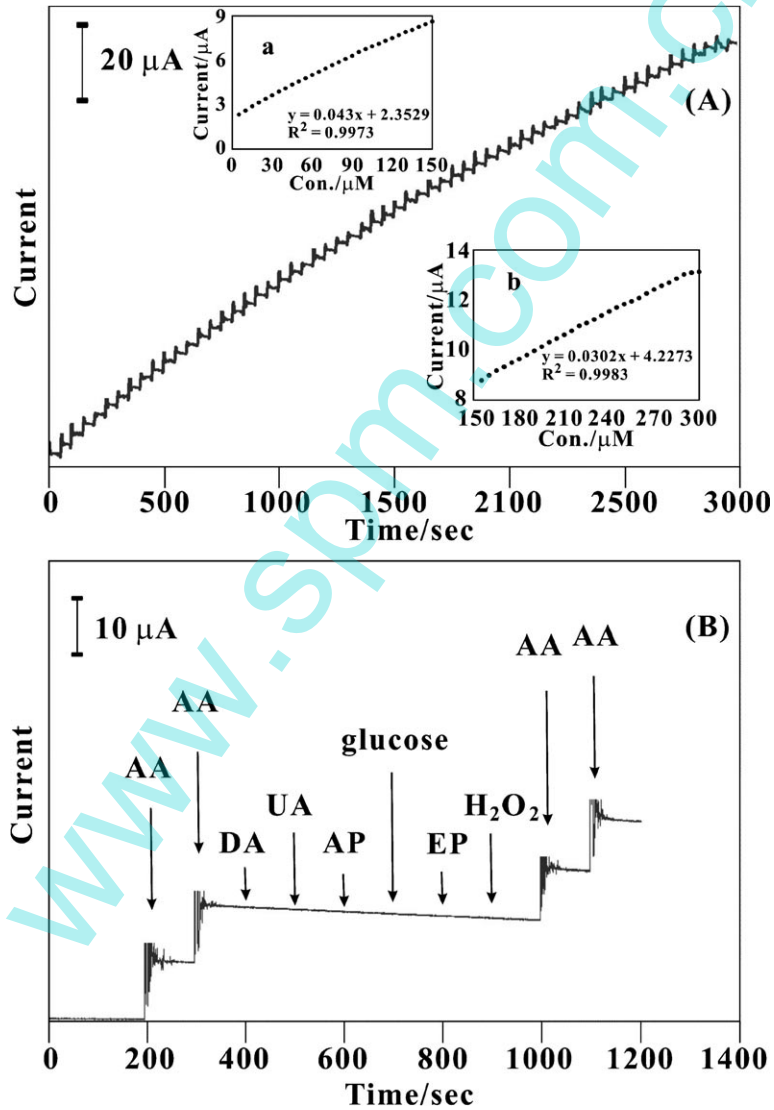

Fig. 5. (A) Typical amperometric curve obtained for a NiHCF-PEDOT/GCE in 0.1 M PBS (pH 7.0) at 0.2 V. Stirring rate 1000 rpm. Successive additions of AA in the range 5×10^{-6} to 3×10^{-4} M ($S/N = 3$). Inserts a and b show the corresponding calibration plots with the concentration of AA between 5×10^{-6} to 1.5×10^{-4} M and 1.55×10^{-4} to 3×10^{-4} M. (B) Typical amperometric curve obtained for a NiHCF-PEDOT/GCE in 0.1 M PBS (pH 7.0) at 0.2 V. Successive additions of (a) 15 μM AA, (b) 15 μM AA, (c) 10 μM DA, (d) 10 μM UA, (e) 10 μM AP, (f) 10 μM glucose, (g) 10 μM EP, (h) 10 μM H_2O_2, (i) 15 μM AA, and (j) 15 μM AA.

Table 1. A comparison of the efficiency of the metal complex mediator-doped-polymer film electrodes used in the AA determination. *LCR*: linear concentration range.

Modified electrode	Method	E_p (mV)	Electrolyte	*LCR* (M)	Sensitivity (A mM^{-1})	Reference
$Fe(CN)_6^{3-/4-}$-PPy/GCE	CV	–	pH 4 glycine buffer	$5\times10^{-4}-1.6\times10^{-2}$	3.1	[43]
NiHCF/PMo/GCE	Amperometric	+500 (SCE)	0.2 M NaCl buffer (pH 1.5)	$1\times10^{-3}-6\times10^{-3}$	–	[38]
$Fe(CN)_6^{3-/4-}$-Tosflex/GCE	Amperometric	+300 (Ag/AgCl)	pH 5 PBS	$1\times10^{-5}-5\times10^{-5}$	26	[44]
$Fe(CN)_6^{3-/4-}$-PEDOT/GCE	CV	+100 (Ag/AgCl)	pH 7 PBS	$2\times10^{-3}-1.6\times10^{-3}$	–	[34]
	Chronoamperometric	–	pH 7 PBS	$2\times10^{-4}-3.2\times10^{-3}$	–	
$Mo(CN)_8^{3-/4-}$-GA-PLL/GCE	Amperometric	+575 (Ag/AgCl)	0.1 M H_2SO_4	$5\times10^{-5}-1.2\times10^{-3}$	15	[45]
$Fe(CN)_6^{3-/4-}$-PPy/CPE	CV	–	pH 7 PBS	$4.5\times10^{-4}-9.6\times10^{-3}$	–	[46]
NiHCF-PEDOT/GC	Amperometric	+200 (Ag/AgCl)	pH 7 PBS	$5\times10^{-6}-3\times10^{-4}$	54	This work

good linear response for the electrocatalytic oxidation of AA in the range 5×10^{-6} to 3×10^{-4} M, and the detection limit was 1×10^{-6} M ($S/N=3$). The linear range and sensitivity observed with the NiHCF-PEDOT/GCE electrode were generally comparable with those of most of the modified electrodes reported in the literature [34, 38, 43–46] (Table 1). The highest linear concentration range (*LCR*) of a NiHCF-PEDOT/GCE modified electrode, compared with that of a NiHCF/PMo/GCE electrode [38] and a $Fe(CN)_6^{3-/4-}$-PEDOT/GCE electrode [34], may be the result of the NiHCF film being bound to the PEDOT film on electrode's surface. Similarly, a NiHCF-PEDOT/GCE modified electrode for the detection of AA also has a higher sensitivity.

The selectivity and potential interference on the NiHCF-PEDOT hybrid film modified electrode were tested using an amperometric technique. In the amperogram shown in Figure 5B, amperometric responses were obtained by successive injection of (a) 15 μM AA, (b) 15 μM AA, (c) 10 μM DA, (d) 10 μM UA, (e) 10 μM AM, (f) 10 μM glucose, (g) 10 μM EP, (h) 10 μM H_2O_2, (i) 15 μM AA, and (j) 15 μM AA. Data were recorded in a stirred 0.1 M PBS solution (pH 7.0) at the same working potential as used for AA (+0.2 V). Results clearly indicated that DA, UA, etc. exhibit non-obvious interference in the steady state current of AA at +0.2 V. This may be attributed to the lower working potential (+0.2 V) used for the oxidation of AA promoted by the NiHCF-PEDOT hybrid film modified electrode.

3.5. Stability and Reproducibility

The reproducibility of the current response of the biosensor was examined by measuring the AA concentration of 1×10^{-4} M, and the relative standard deviation was determined to be 2.64 ($n=5$), showing that the biosensor possessed a good reproducibility. In addition, to determine the catalytic current response during the oxidation of AA, the NiHCF-PEDOT/GCE electrode was tested in a solution containing 1×10^{-4} M of AA, before and after continuously stirring the buffered solution for a period of 30 min. The response of the electrode signal showed no significant change before and after stirring the solution. This test indicated that reproducible results could be obtained using the NiHCF-PEDOT/GCE electrode. The stability of NiHCF-PEDOT hybrid film modified electrode was then investigated by storing it at room temperature in the presence and absence of PBS (pH 7.0). It was stable for one month but thereafter there was a gradual decrease (10%) in the current values. When the NiHCF-PEDOT hybrid film modified electrode store for a week in pure 0.1 M PBS (pH 7.0), the voltammetric response current of AA decreased by 9% of the initial current. These results suggest that the NiHCF-PEDOT/GCE has high stability and good reproducibility.

4. Conclusions

A NiHCF-PEDOT hybrid film was successfully electrodeposited on a GCE. The NiHCF-PEDOT hybrid film was characterized using AFM, FE-SEM, EDS, EIS, and XRD. The advantages of the NiHCF-PEDOT hybrid film were demonstrated for the sensing of AA in the presence of major interferences, such as DA and UA. The hybrid film modified electrode displays a linear response from 1×10^{-5} to 1.8×10^{-4} M AA, with a correlation coefficient of 0.964. The detection limit was found to be 1×10^{-6} M and the response time was 3 s. This new method can be applied for the electroanalysis of AA.

Acknowledgement

This work was supported by The National Science Council of Taiwan.

References

[1] E. Raveh, T. Saban, H. Zipia, Y. E. Beit, *J. Sci. Food Agric.* **2009**, *89*, 1825.
[2] L. Novakova, P. Solich, D. Solichova, *Trends Anal. Chem.* **2008**, *27*, 10.
[3] R. Jariwalla, S. Harakeh, L. Packer, J. Fuchs, *Vitamin C in Health and Disease*, Marcel Dekker, New York **1997**, p. 309.

[4] S. Harakeh, R. Jariwalla, *AIDS Res. Hum. Retroviruses* **1997**, *13*, 235.
[5] C. Tsao, W. Dunham, P. Leung, *Cancer J.* **1995**, *8*, 157.
[6] J. Wenrui, J. Lei, *Electrophoresis* **2002**, *23*, 2471.
[7] S. Thiagarajan, T. H. Tsai, S. M. Chen, *Biosens. Bioelectron.* **2009**, *24*, 2712.
[8] H. R. Zare, N. Nasirizadeh, M. Mazloum-Ardakani, *J. Electroanal. Chem.* **2005**, *577*, 25.
[9] A. Balamurugan, S. M. Chen, *Anal. Chim. Acta* **2007**, *596*, 92.
[10] J. Mathiyarasu, S. Senthilkumar, K. L. N. Phani, V. Yegnaraman, *Mater. Lett.* **2008**, *62*, 571.
[11] S. Harish, J. Mathiyarasu, K. L. N. Phani, V. Yegnaraman, *J. Appl. Electrochem.* **2008**, *38*, 1583.
[12] M. A. Dayton, A. G. Ewing, R. M. Wightman, *Anal. Chem.* **1980**, *52*, 2392.
[13] H. R. Zare, N. Nasirizadeh, M. Mazloum-Ardakani, *J. Electroanal. Chem.* **2005**, *577*, 25.
[14] J. H. Roe, *J. Biol. Chem.* **1961**, *236*, 1611.
[15] M. A. Farajzadeh, S. Nagizadeh, *J. Anal. Chem.* **2003**, *58*, 927.
[16] R. T. Perez, L. C. Martinez, V. Tomas, J. Fenol, *Analyst* **2001**, *126*, 1436.
[17] M. C. Yebra, R. M. Cespon, C. A. Moreno, *Anal. Chim. Acta* **2001**, *448*, 157.
[18] F. O. Silva, *Food Control* **2005**, *16*, 55.
[19] K. P. Emadi, Z. Verjee, A. V. Levin, K. Adeli, *Clin. Biochem.* **2005**, *38*, 450.
[20] E. Onelli, A. Mosca, *Life Chem. Rep.* **1994**, *110*, 189.
[21] Q. L. Sheng, H. Yu, J. B. Zheng, *Electrochim. Acta* **2007**, *52*, 4506.
[22] M. Noroozifar, M. K. Motlagh, A. Taheri, *Talanta* **2009**, in press.
[23] R. Hosseinzadeh, R. E. Sabzi, K. Ghasemlu, *Colloids Surf. B, Biointerf.* **2009**, *68*, 213.
[24] Z. Xun, C. Cai, W. Xing, T. Lu, *J. Electroanal. Chem.* **2003**, *545*, 19.
[25] D. M. Zhou, H. X. Ju, H. Y. Chen, *J. Electroanal. Chem.* **1996**, *408*, 219.
[26] R. Pauliukaite, M. E. Ghica, C. M. A. Brett, *Anal. Bioanal. Chem.* **2005**, *381*, 972.
[27] R. Vittal, H. Gomathi, K. J. Kim, *Adv. Colloid Interf. Sci.* **2006**, *119*, 55.
[28] A. L. Oleksiak, A. P. Nowak, *J. Power Sources* **2007**, *173*, 829.
[29] J. Balmaseda, E. Reguera, J. R. Hernandez, L. Reguera, M. Autie, *Micropor. Mesopor. Mater.* **2006**, *96*, 222.
[30] C. Barbero, M. C. Miras, B. Schryder, O. Hass, R. Kotz, *J. Mater. Chem.* **1994**, *4*, 1775.
[31] N. Oyama, T. Tatsuma, T. Sato, T. Sotomura, *Nature (London)* **1995**, *373*, 598.
[32] G. Inzelt, M. Pineri, J. W. Schultze, M. A. Vorotyntsev, *Electrochim. Acta* **2000**, *45*, 2403.
[33] E. M. Genies, A. Boyle, M. Lapkowski, C. Tsintavis, *Synth. Met.* **1990**, *36*, 139.
[34] V. S. Vasantha, S. M. Chen, *Electrochim. Acta* **2005**, *51*, 347.
[35] V. S. Vasantha, S. M. Chen, *J. Electroanal. Chem.* **2006**, *592*, 77.
[36] S. Sinha, B. D. Humphrey, A. B. Bocarsly, *Inorg. Chem.* **1984**, *23*, 203.
[37] S. M. Chen, *J. Electroanal. Chem.* **2002**, *521*, 29.
[38] S. M. Chen, C. Y. Liou, A. Balamurugan, R. Thangamuthu, *Electroanalysis* **2009**, *21*, 919.
[39] Q. Kong, X. Chen, J. Yao, D. Xue, *Nanotechnology* **2005**, *16*, 164.
[40] W. A. Steen, S. W. Han, Q. Yu, R. A. Gordon, J. O. Cross, E. A. Stern, G. T. Seidler, K. M. Jeerage, D. T. Schwartz, *Langmuir* **2002**, *18*, 7714.
[41] W. A. Steen, D. T. Schwartz, *Chem. Mater.* **2003**, *15*, 2449.
[42] R. W. Murray, in *Electroanalytical Chemistry*, Vol. 13 (Ed: A. J. Bard), Marcel Dekker, New York **1984**, p. 191.
[43] M. H. Pournaghi-Azar, R. Ojani, *J. Solid State Electrochem.* **2000**, *4*, 75.
[44] J. M. Zen, D. M. Tsai, A. S. Kumar, V. Dharuman, *Electrochem. Commun.* **2000**, *2*, 782.
[45] R. Thangamuthu, Y. C. Wu, S. M. Chen, *Electroanalysis* **2009**, *21*, 165.
[46] J. B. Raoof, R. Ojani, S. R. Nadimi, *Electrochim. Acta* **2004**, *49*, 271.